Numerical simulations in stochastic mechanics

Marvin McClendon
Program in Applied Mathematics, Princeton University, Princeton, New Jersey 08544

Herschel Rabitz
Department of Chemistry, Princeton University, Princeton, New Jersey 08544
(Received 20 July 1987)

The stochastic differential equation of Nelson's stochastic mechanics is integrated numerically for several simple quantum systems. The calculations are performed with use of Helfand and Greenside's method and pseudorandom numbers. The resulting trajectories are analyzed both individually and collectively to yield insight into momentum, uncertainty principles, interference, tunneling, quantum chaos, and common models of diatomic molecules from the stochastic quantization point of view. In addition to confirming Shucker's momentum theorem, these simulations illustrate, within the context of stochastic mechanics, the position-momentum and time-energy uncertainty relations, the two-slit diffraction pattern, exponential decay of an unstable system, and the greater degree of anticorrelation in a valence-bond model as compared with a molecular-orbital model of H_2. The attempt to find exponential divergence of initially nearby trajectories, potentially useful as a criterion for quantum chaos, in a periodically forced oscillator is inconclusive. A way of computing excited energies from the ground-state motion is presented. In all of these studies the use of particle trajectories allows a more insightful interpretation of physical phenomena than is possible within traditional wave mechanics.

I. INTRODUCTION

Nelson's stochastic mechanics[1-4] is a theory in which quantum phenomena are described in terms of conservative diffusion processes rather than wave functions. Although the Schrödinger equation can be derived within the theory and has utility as an aid in carrying out calculations, it is not the equation of motion,[5] just as the wave function is not the basic dynamical object. Instead, the fundamental mechanical equation for a given quantum phenomenon is a stochastic differential equation whose dependent variable represents the position and whose independent variable stands for time, just as in the case of Newtonian dynamics. A physical system is assumed to undergo a diffusion whose properties depend not only on the potential but also on the wave function itself. The solution of the stochastic differential equation is a stochastic process on configuration space, and its probability density is identical to that obtained by squaring the modulus of the normalized wave function. Since all experimental measurements ultimately reduce to position measurements, stochastic mechanics therefore makes the same observable predictions as ordinary quantum mechanics,[4,6] and thus is experimentally indistinguishable from it.

A significant feature of stochastic quantization is that, in stark contrast to conventional quantum theory, it provides not only a probability distribution of possible configurations at each time but also actual continuous configuration trajectories as functions of time[7] (i.e., the sample paths of the diffusion). Stochastic mechanics can be viewed as a recasting of the Feynman path integral theory.[8,9] Studying the sample trajectories, which are the same as Feynman's paths, as realizations of a diffusion process, can yield insight into the behavior of quantum systems; moreover, the theory affords new computational means for looking at topics such as scattering[3,10] and quantum chaos.[11,12]

Stochastic quantization and its ramifications have received increasing attention in recent years. This work has been almost entirely foundational or analytical. An exception is the qualitative numerical study of quantum kinematics from the stochastic point of view in Ref. 13. The latter-mentioned paper is a forerunner of our own computer investigations. We hope to demonstrate further the feasibility and usefulness of computational research employing the concepts and tools provided by Nelsons's theory.

The remainder of the paper is organized as follows. Section II briefly explains some theoretical background and the numerical technique used in the calculational studies which are reported on subsequently. The computational part comprises investigations of momentum and uncertainty principles in free motion (Sec. III), interference (Sec. IV), tunneling (Sec. V), quantum chaos (Sec. VI), and one-dimensional models of diatomic two-electron molecules (Sec. VII). Finally, in Sec. VIII we consider the information about excited states that can be gained by looking at the motion of the ground state. Section IX summarizes and concludes the article.

II. THEORY AND METHODOLOGY

The central assertion of stochastic mechanics is that to a normalized solution ψ of the time-dependent Schrödinger equation there is associated a Markovian

diffusion process satisfying the Langevin stochastic differential equation[14,15]

$$dq(t)-b(q(t),t)dt+\sqrt{2\nu}\,dw(t) \tag{1}$$

with diffusion coefficient

$$\nu=\frac{\hbar}{2m}\ , \tag{2}$$

forward drift

$$b(x,t)=\frac{\hbar}{m}\left[\mathrm{Re}\left[\frac{\nabla\psi}{\psi}\right]+\mathrm{Im}\left[\frac{\nabla\psi}{\psi}\right]\right]\ , \tag{3}$$

and probability density

$$\rho(x,t)=|\psi(x,t)|^2\ . \tag{4}$$

This correspondence goes both ways,[4] and Carlen[2,3] has rigorously proved the existence of the Nelson diffusion process with drift and density given by (3) and (4), respectively, for a wide class of potentials and wave functions.

We have employed the procedure of Helfand and Greenside[16,17] to generate and analyze representative approximate trajectories for the Langevin equation (1) describing certain quantum systems. Other approaches are mentioned by Wright.[18] The utilization of such methods here presupposes that we already have an exact or approximate wave function for the system in question, and thus, via (3), an expression for the drift. Therefore, the present calculations are performed mainly for the insight they give into quantum behavior.

The technique of Helfand and Greenside is an extension of the familiar Runge-Kutta method for deterministic ordinary differential equations, which seeks to match the Taylor series of the solution about a given mesh point up through a given order so as to estimate the solution at the next mesh point to that order of accuracy.[16] The stochastic version is obtained by writing the Langevin equation in integrated form and expanding the right-hand side in a power series in the square root of the time increment, where the order of the explicitly stochastic terms is determined in a probabilistic sense by the order of the corresponding moments. The method extrapolates from one mesh point to the next by evaluating the drift function at certain sets of stochastically determined points and then taking a linear combination of these values plus another random term. We use a generalization of the second-order method presented by Helfand in Ref. 16.

For the sake of simplicity we take the initial-time mesh point to be $t=0$. The second-order Helfand-Greenside algorithm for q is then

$$\begin{aligned} g_1&=b(q(0)+\lambda_1(2\nu)^{1/2}(\delta t)^{1/2}Z,0)\ ,\\ q_2&=b(q(0)+\beta g_1\delta t+\lambda_2(2\nu)^{1/2}(\delta t)^{1/2}Z,\delta t)\ ,\\ q(\delta t)&=q(0)+\delta t(A_1g_1+A_2g_2)+\lambda_0(2\nu)^{1/2}(\delta t)^{1/2}Z\ , \end{aligned} \tag{5}$$

where Z is a Gaussian random variable with mean zero and variance unity, realizations of which are provided by practice by a pseudorandom number generator, and where A_1, A_2, β_0, λ_0, λ_1, and λ_2 are the as yet unspecified parameters. We use the following values for these parameters, which result in (5) matching the exact solution up through second order in δt:[16]

$$A_1=A_2=\tfrac{1}{2},\quad \beta=1,\quad \lambda_0=\lambda_2=1,\quad \lambda_1=0\ . \tag{6}$$

Thus the only things that need to be supplied now in order to utilize (5) are the drift function $b(x,t)$ and the distribution of the initial points of the trajectories.

Although the behavior of a single sample trajectory can be illuminating (see Ref. 13), achieving a full picture of the physical system often requires the examination of many trajectories. This is particularly true if one is interested in average or expected quantities. In the sections below we shall have occasion to estimate the mean $E[\phi[q]]$ of a functional of the process q solving (1) by evaluating it for finitely many numerically generated sample paths and then taking the average of this set of numbers.

In doing so we assume that the following limit holds:[19]

$$E[\phi[q]]=\lim_{N\to\infty}\left[\frac{1}{N}\sum_{a=1}^{N}\phi[q^{(a)}]\right]\ . \tag{7}$$

Here the index a on the right-hand side labels individual sample trajectories. Then by taking a large enough number of sample paths, the true expectation can be estimated arbitrarily accurately.

The calculations in this work were performed on a Digital Equipment Corporation VAX11/780 computer. IMSL library routines, mainly the Gaussian pseudorandom number generators GGNPM and GGNQF, were employed.

Discretizing a diffusion process entails approximating it as a random walk; in our computer modeling a quantum particle undergoes a random walk in which the expected value of the square of the spatial step size is equal to the time increment multipled by the diffusion coefficient. Furthermore, it is clear from the relationship (3) between the drift and the wave function, and between the wave function and the potential, that a stochastic mechanical particle will tend to spend more time where the potential is lower and less where it is higher, resulting in a higher density in the former regions and a lower density in the latter ones. This is related to a random-walk technique which Anderson[20] and others have used to solve the Schrödinger equation approximately.

III. FREE MOTION

Utilizing a simple finite-difference scheme, Yasue and Zambrini[13] have studied the kinematics of single free-particle trajectories. In this section we make use of the more sophisticated numerical method mentioned above to compute many trajectories for a system undergoing free motion, taking a Gaussian wave packet as the wave function. We examine the long-time behavior of a single trajectory and also the average behavior of an ensemble of trajectories, comparing what happens with some of the rigorous results obtained by other workers, primarily concerning linear momentum and uncertainty principles.

In Ref. 21 Shucker showed that the sample paths for a system with zero potential behave asymptotically, as

$t \to \infty$, like the trajectories of the corresponding classical system. Specifically, he proved that under mild assumptions on a solution $\psi(x,t)$ of the free Schrödinger equation (henceforth we use units of $\hbar = m = 1$, unless otherwise stated), the limit

$$p = \lim_{t \to \infty} \left[\frac{q(t) - q(0)}{t} \right] \tag{8}$$

exists for almost every sample path of the Nelson process determined by this wave function and that, moreover, the probability density of this limit is given by

$$\rho_p(p) = |\tilde{\psi}(p)|^2 , \tag{9}$$

where $\tilde{\psi}$ is the spatial Fourier transform of $\psi(x,0)$. p would be exactly equal to the velocity in a free Newtonian system.[21] Zero potential implies zero stochastic acceleration,[6,22] and therefore one is justified in considering (8) to be a definition of momentum for a freely evolving stochastic mechanical system, even at finite times; each individual sample trajectory then has its own constant momentum. Biler[10] and Carlen[2,3] have extended these results to systems with interaction, under some restrictions.

We start with the initial wave function

$$\psi(x,0) = \frac{1}{\pi^{1/4}} \exp\left[-\frac{x^2}{2} \right] e^{ikx} \tag{10}$$

in configuration space, representing a Gaussian probability distribution with mean 0 and variance 0.5 whose center moves to the right at uniform speed k. The freely propagating wave packet is then

$$\psi(x,t) = \frac{1}{\pi^{1/4}} \frac{1}{\sqrt{1+it}} \exp\left[-\frac{(1-it)(x-kt)^2}{2(1+t^2)} + ik\left[x - \frac{kt}{2} \right] \right] . \tag{11}$$

Substituting (11) into formula (3), we get the forward drift function

$$b(x,t) = k + \frac{(t-1)(x-kt)}{1+t^2} , \tag{12}$$

to be inserted into (1). Letting $k = 10$ and using the algorithm (5), we calculated four individual sample paths, each with initial point $q(0) = 1$ and time step size $\delta t = 0.01$, for a total of 100 000 iterations, or 1000 units of time. The values of $q(t)/t$ for the last 100 points on each of these trajectories were examined and found to have settled down to the limits 2.003 598, 0.491 235, 0.768 458, and 1.809 877, respectively. For each path we used a different seed for the pseudorandom number generator, but otherwise the conditions governing their evolution were identical. Different individual trajectories led to different values of the limit (8) despite coming from the same wave function and identical initial points; this is not surprising, for although the value of (8) is completely independent of $q(0)$, it is a random quantity, with probability distribution (9).

Again taking $k = 10$, we next generated an ensemble of 10 000 trajectories of (1) and (12), distributing the initial positions $q(0)$ according to the probability density

$$\rho_0(x) = |\psi(x,0)|^2 = \frac{1}{\sqrt{\pi}} \exp(-x^2) \tag{13}$$

by employing a Gaussian pseudorandom number generator. After all of these trajectories evolved for 100 units of time, with time step size $\delta t = 0.01$, we counted how many final values $q(100)/100$ lie in the bins

$$6.8 + \frac{2}{225} n < \frac{q(100)}{100} \le 6.8 + \frac{2}{225}(n+1) \quad \text{for } n = 0, 1, \ldots, 719 ,$$

the latter intervals having been chosen to cover all these momentum values and to give a reasonable resolution. The result is plotted in Fig. 1; this gives the approximate distribution of particle momenta at time $t = 100$. The overall shape of the curve is that of a Gaussian. The sample mean and standard deviation turn out to be, respectively,

$$\left\langle \frac{q(100)}{100} \right\rangle_{\text{sample}} = \frac{\sum_{a=1}^{10\,000} \frac{q^{(a)}(100)}{100}}{10\,000} = 9.9885 \tag{14}$$

and

$$\left[\Delta \frac{q(100)}{100} \right]_{\text{sample}} = \frac{\sum_{a=1}^{10\,000} \left[\frac{q^{(a)}(100)}{100} - \left\langle \frac{q(100)}{100} \right\rangle_{\text{sample}} \right]^2}{9999} . \tag{15}$$

The theoretical probability density at $t = 100$ is Gaussian with mean $k = 10$ and standard deviation

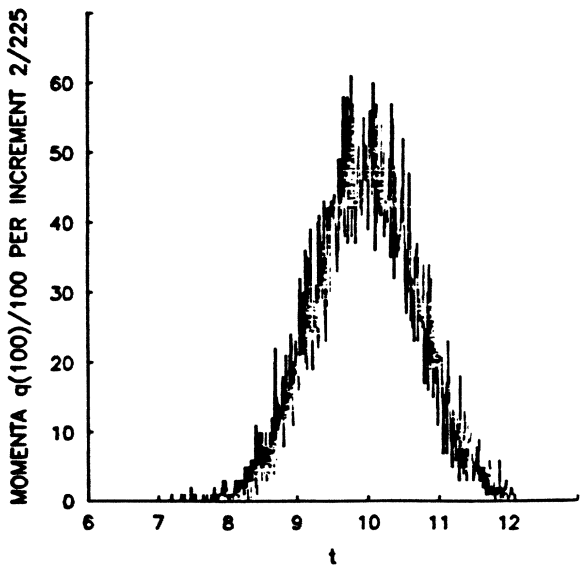

FIG. 1. For free particle dynamics, number of final approximate momentum values $q(100)/100$ per bin of length 2/225, where 10 000 trajectories of $q(t)$ are calculated with time increment 0.01 from initial Gaussian distribution with mean 0 and variance 0.5.

$$\Delta\left[\frac{q(100)}{100}\right]=0.707\,42\ .$$

Our results accord quite well with these values; the mean of Fig. 1 is well fitted by

$$\rho_p(p,100)=\frac{1}{\sqrt{\pi}}e^{-(p-10)^2}\ . \tag{16}$$

The standard position-momentum uncertainty principle has been rederived within stochastic mechanics; furthermore, it has been shown that this relation follows from a more stringent uncertainty inequality in which the momentum uncertainty is replaced by the part of it due solely to the uncertainty in the osmotic velocity.[4,23,24] Golin[25] has derived another stronger form of the position-momentum uncertainty principle in stochastic mechanics (equivalent to a quantum-mechanical version of Schrödinger[26]) by adding the inequality $(\Delta q)(\Delta v)\geq \mathrm{Cov}^2(q,v)$ to the position-osmotic velocity uncertainty inequality just mentioned; here $\mathrm{Cov}(q,v)$ denotes the covariance of the position q and the current velocity v.[4] We write the latter strengthened inequality in the form

$$(\Delta q)(\Delta p)\geq[\mathrm{Cov}^2(q,p)+\tfrac{1}{4}]^{1/2}\ . \tag{17}$$

(The term $\frac{1}{4}$ corresponds to the square of $\hbar/2$.) We consider the same set of 10 000 trajectories generated above, with $\delta t=0.01$ and initial distribution (13). Observing that the momentum at time $t=100$ is approximated, via Shucker's theorem, by $q(100)/100$, the sample root mean-square deviation of $q(100)$ is just 10 times the result in (15), namely, $\Delta q(100)=72.984\,33$. The sample covariance at $t=100$, the sum of the products of position minus its mean and momentum minus its mean for all the trajectories divided by the number of them, is computed to be $\mathrm{Cov}(q(100),p(100))=53.2617$. We find that

$$[\Delta q(100)]_{\text{sample}}\left[\Delta\left[\frac{q(100)}{100}\right]\right]_{\text{sample}}$$

$$=53.268>53.264$$

$$=[\mathrm{cov}^2(q(100),q(100)/100)+\tfrac{1}{4}]^{1/2}\ . \tag{18}$$

The left-hand side is only slightly larger than the right-hand side, and we have essentially an equality (we are dealing with a minimum-uncertainty wave packet). Thus the stronger form (17) of the position-momentum uncertainty relation is satisfied by this ensemble of approximate sample paths.

Next we use the same process, with the same initial distribution (13), to calculate the standard deviation of the first-passage times of a sequence of freely moving particles past a specified point and verify, with this time uncertainty and with the energy spread defined in terms of the quantum-mechanical momentum distribution, that the time-energy uncertainty principle[27] is fulfilled. This provides another way to look at the relationship between arrival time and energy distributions in nonrelativistic quantum phenomena.

Farina[28] defines arrival, departure, and transit times (with respect to a certain point) for a free quantum particle in a probabilistic manner. Using the Mandelstam-Tamm inequality he shows that the transit time and the standard deviation of the energy satisfy the time-energy uncertainty principle. For comparison with this, we compute the particle's time of first passage[15] of the detection point for each of the sample trajectories and compute the mean and standard deviation of this set of times. In analogy with Farina's work, the transit time is defined here as twice the standard deviation of the first-passage times. In the stochastic mechanical approach the particle has a trajectory which reaches the given point at some (random) time. The particle will pass the point in opposite directions infinitely often due to fluctuations on arbitrarily small time scales, but on any finite time scale this phenomenon is not seen and the particle can be treated as simply passing the point in a smooth way.

We take the expected drift $k=10$, which here is equal to the mean momentum in both quantum mechanics and, via Shucker's theorem,[21] in stochastic mechanics, large enough so that the wave function will move to the right faster than it spreads out. Choosing the detection point to be $x=5$, we integrated each of 10 000 approximate trajectories of (1) with drift (12), initial distribution (13), and time increment $\delta t=0.01$, until this point was reached. The average of this sample of detection times is $t=0.502\,98$, which agrees well with the time $t=0.5$ when the center of the spreading Gaussian distribution of (11) arrives at $x=5$. The standard deviation of the sample of times we found to be $\delta t=0.094\,97$.

Now we use the quantum-mechanical momentum distribution, which is time dependent, to calculate the standard deviation of the energy. This is justified because Shucker's theorem allows the ordinary quantum momentum distribution to be considered in the free case as the momentum distribution in stochastic mechanics. Employing the momentum distribution (9), we first find the mean to be $E[\varepsilon]=\frac{1}{4}+k^2/2$. We can then calculate the energy variance,

$$(\Delta\varepsilon)^2=\frac{1}{8}+\frac{k^2}{2}\ . \tag{19}$$

The energy uncertainty with $k=10$ is $\Delta\varepsilon=50.125$. Multiplying this by the first-passage-time standard deviation computed earlier, we have

$$(\Delta t)(\Delta\varepsilon)=0.682\,93>\tfrac{1}{2}\ . \tag{20}$$

This latter inequality implies that the time-energy uncertainty principle is fulfilled.

IV. DOUBLE-SLIT DIFFRACTION PROBLEM

The phenomenon we examine in this section is actually another instance of free motion with the initial wave function being the sum of two narrow Gaussians with separate centers. This quantum system furnishes a model of the two-slit diffraction experiment, where each Gaussian plays the role of a source at one of the slits.[6,13,22] Although the physical phenomenon itself is spatially two dimensional, in this model we consider only the y direction

along the line joining the Gaussian "slits." Thus the motion perpendicular to the barrier and screen is modeled by classical motion at a uniform constant speed. Hence, because fluctuations in this direction are neglected and also because the initial wave function is not exactly that corresponding to actual physical slits, the resulting interference pattern may differ slightly from that obtained in a real experiment. The distances between successive interference peaks and troughs, however, will be the same.

In their paper,[13] Yasue and Zambrini looked at the kinematics of individual stochastic mechanical trajectories for an approximation to the wave function that we shall be considering. Using de Broglie and Bohm's quantum potential theory, Philippidis, Dewdney, and Hiley[29] calculated an ensemble of trajectories for the two-slit problem, demonstrating how the quantum potential causes a clustering of particle paths leading to the well-known interference pattern even though each path actually passes through one or the other of the slits. Nelson[6,22] has proved that an interference pattern will result in the two-slit experiment in stochastic mechanics; we propose to demonstrate this interference pattern from an ensemble of numerically generated stochastic mechanical trajectories and compare it with the theoretical probability density. In addition, we shall analyze a set of sample paths that all go through just one slit even though both are open.

Beginning at $t=0$, with the wave function

$$\psi(y,0)=\frac{1}{\left\{2\sqrt{\pi}\left[1+\exp\left[-\frac{s^2}{a}\right]\right]\right\}^{1/2}}\times\left[\exp\left[\frac{-(y+s)^2}{2a}\right]+\exp\left[\frac{-(y-s)^2}{2a}\right]\right] \tag{21}$$

for some suitably small-width parameter a and separation parameter s (assume $a<s$), we solve the one-dimensional free Schrödinger equation, obtaining the normalized wave function

$$\psi(y,t)=\frac{1}{(2\sqrt{\pi})^{1/2}}\frac{1}{\sqrt{a+it}}\left[\frac{a}{1+\exp\left[\frac{-s^2}{a}\right]}\right]^{1/2}\times\left[\exp\left[\frac{-(a-it)(y+s)}{2(a^2+t^2)}\right]^2+\exp\left[\frac{-(a-it)(y-s)}{2(a^2+t^2)}\right]^2\right]. \tag{22}$$

Applying the formula (3) for the forward drift now yields the expression

$$b(y,t)=(\mathrm{Re}+\mathrm{Im})\left\{\frac{-(a-it)}{a^2+t^2}\left[(y+s)\exp\left[\frac{-(a-it)(y+s)^2}{2(a^2+t^2)}\right]+(y-s)\exp\left[\frac{-(a-it)(y-s)^2}{2(a^2+t^2)}\right]\right]\times\left[\exp\left[\frac{-(a-it)(y+s)^2}{2(a^2+t^2)}\right]+\exp\left[\frac{-(a-it)(y-s)^2}{2(a^2+t^2)}\right]\right]\right\}. \tag{23}$$

Taking the square of the modulus of (22) gives the probability density

$$\rho(y,t)=\frac{a}{2\left\{\pi(a^2+t^2)\left[1+\exp\left[\frac{-s^2}{a}\right]\right]\right\}^{1/2}}\left[\exp\left[\frac{-a(y+s)^2}{a^2+t^2}\right]+\exp\left[\frac{-a(y-s)^2}{a^2+t^2}\right]+2\exp\left[\frac{-a(y^2+s^2)}{a^2+t^2}\right]\cos\left[\frac{2tsy}{a^2+t^2}\right]\right]. \tag{24}$$

For $t\gg s$, the drift is enormous near the lines $y=(2n+1)\pi t/2s$ in the (t,y) plane and points away from them.[22] Hence, as can be shown from (24), the separation between minima of ρ is approximately $\pi t/s$ at time t. Letting $s=1$ and $a=0.01$ makes the cross terms in the absolute square of (22) negligible and we can take the initial probability density to be the sum of two Gaussians. Distributing half the initial points on each Gaussian, we integrated 10 000 trajectories for (2) with drift (23) and with time step size $\delta t=0.001$ from $t=0$ to $t=1$. Counting the number of final y values in each bin

$$n\frac{\pi}{240}<y\le(n+1)\frac{\pi}{40}\quad\text{for } n=-360,-359,\ldots,359,$$

the intervals having been selected to cover the relevant region and to provide sufficient resolution, we get the in-

terference pattern plotted in Fig. 2(a). For the purpose of comparison we graph the theoretically predicted diffraction pattern (24) at $t=1$ in Fig. 2(b). Clearly the distances between the peaks and troughs in Fig. 2(a) are correct, and the relative heights of the intensity peaks also agree well with those in Fig. 2(b).

The fringe pattern in Fig. 2(a) comes from a finite number of well-defined stochastic particle trajectories, half of which emerged from one of the slits and half from the other. An interesting question now arises: What happens if we keep the same wave function (22), corresponding to both slits being open, but start all of the trajectories at only one of the Gaussian slits, say, the one centered at $y=1$? It is evident[22] that an interference pattern will again be obtained, but it will be skewed to the right. This pattern cannot be produced experimentally, since preparing the system physically so that the particle must begin at one of the slits entails closing the other, and there would then be no diffraction.[22] Nevertheless, this phenomenon can be "simulated" mathematically, which involves conditioning the process so that its initial points are all distributed according to the absolute square of the right-hand Gaussian in (23) alone; for this process, the actual probability density is not the absolute square of the wave function. Integrating and analyzing as before 10 000 trajectories for this problem, we obtained in Fig. 3.

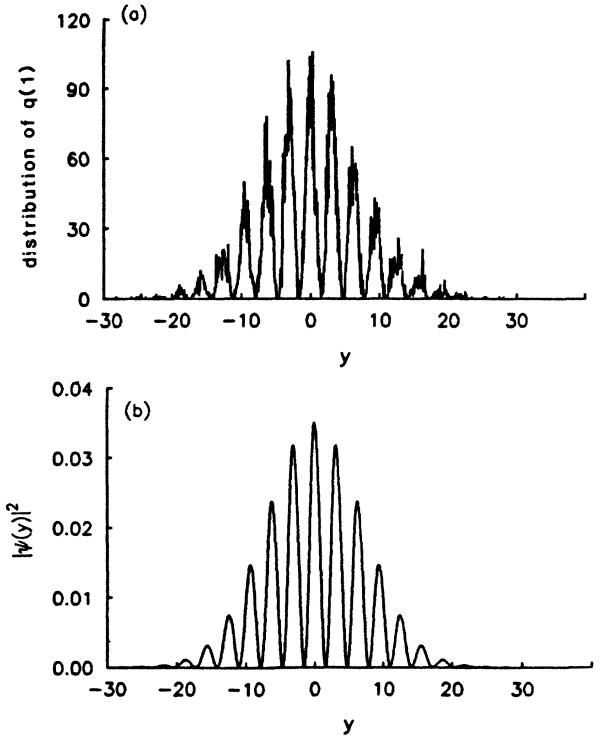

FIG. 2. For the two-slit diffraction problem: (a) the number of final positions $q(1)$ in each bin of length $\pi/40$, where 10 000 trajectories are calculated with time increment 0.001 with 5000 initial values $q(0)$ distributed according to each of two Gaussian "slits" with centers $y=-1$ and $y=1$, respectively, and variance 0.005; (b) graph of absolute square of wave function at time $t=1$.

The distances between peaks and troughs are exactly the same as in Fig. 2(a).

Doing the same thing but starting all the trajectories instead on the left Gaussian yielded the mirror-image skewed diffraction pattern, and taking half the sum of the two skewed patterns produced the pattern in Fig. 2(a) again. This is not surprising, for the two-slit process is an equally weighted mixture of the two corresponding processes conditioned to begin solely at one or the other of the slits.

The spacings among the various maxima and minima in these diffraction patterns are determined entirely by the drift (23), which is uniquely specified by the wave function (22). (The relative heights are determined by the initial density.) This is analogous to the situation in Bohm's approach,[29] where the interference pattern is an effect of the quantum potential, which in turn is determined by the wave function.

The curves in Figs. 2(a) and 3 represent approximations (up to multiplication by normalizing constants) of the probability density $\rho(y,1)$ at time $t=1$ corresponding to given initial densities $\rho_0(y)=\rho(y,0)$. The propagation forward in time from $t=0$ to $t=1$ of the density is expressed by the Chapman-Kolmogorov equation[9,14,15]

$$\rho(y,t)=\int p(y,t;\eta,0)\rho_0(\eta)d\eta\ , \tag{25}$$

where $p(y,t;\eta,0)$ is the transition probability density. The final density can be viewed as the distribution of points of first exit[15,14] of the diffusion process from the region between the slits and the detection screen. What we have done in this section illustrates a numerical, essentially Monte Carlo, method for calculating the output left-hand side of (25) given the input initial density ρ_0.

We point out that similar stochastic mechanical calcu-

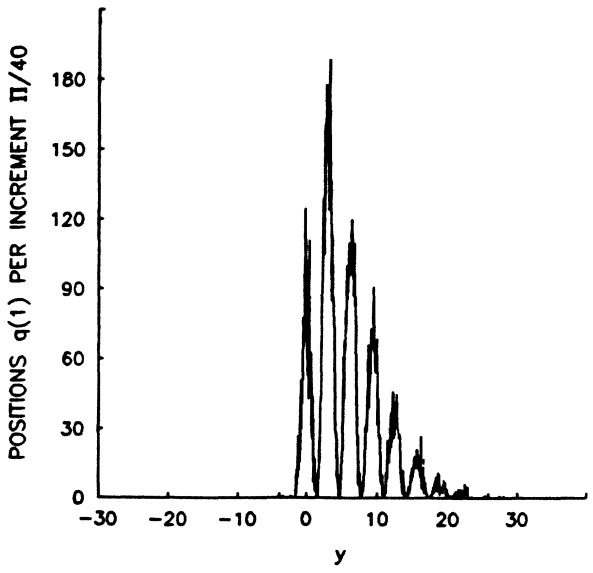

FIG. 3. For the two-slit diffraction problem, the number of final positions $q(1)$ in each bin of length $\pi/40$, where all 10 000 trajectories have initial values $q(0)$ distributed according to the right-hand Gaussian "slit" (centered at $y=1$).

lations could be used to investigate multiple-time phenomena such as the diffraction pattern produced on a screen slanted at an arbitrary angle with respect to the line or plane containing the centers of the slits. Such problems cannot be examined straightforwardly within the theoretical framework of conventional quantum mechanics, and they can be formulated as first-exit problems[14,15] by considering time as another spatial dimension and the extended diffusion with zero diffusion coefficient in that direction. This is analogous to the way that a system of nonautonomous stochastic differential equations can be rewritten as an autonomous system with one more dimension.[17]

V. TUNNELING

Stochastic mechanics, in keeping with its treatment of quantum phenomena in classical terms, yields an intuitively appealing description of quantum tunneling. The energy in stochastic mechanics is a randomly fluctuating quantity which is always non-negative just as in Newtonian mechanics. Thus a stochastic mechanical system never actually "tunnels" through a potential barrier; rather, it is "kicked" over the barrier by a large enough positive energy fluctuation resulting from a configuration fluctuation. This situation is closely analogous to that of a classical particle in a heat bath which must receive an energy fluctuation to cross a potential carrier or to that of a diffusion-driven chemical reaction which must go over an activation energy barrier in order to occur.[15] A similar interpretation of tunneling exists in the quantum potential approach, as Dewdney and Hiley[30] have shown in their study of the crossing of square potential barriers by Bohm-type trajectories.[31]

The problem of analyzing the decay of unstable states in one dimension has been discussed by Jona-Lasinio, Martinelli, and Scoppola.[32] They illustrate how the point of view of stochastic mechanics leads to a natural way of extracting the transient exponential-decay regime. In this section we employ a particular version of their formal type of system to generate an ensemble of 1000 sample trajectories for the decaying quantum state. Then we calculate the decay-time distribution for this sample of paths and show that it is indeed approximately exponential. As in Ref. 32, here the mass is set equal to unity and $\hbar$ is the diffusion parameter.

Our potential is

$$V(x)=\left[1-2\exp\left[-\frac{1}{2\beta}\right]\right]\frac{1}{x}\exp\left[\frac{1-x^2}{2}\right]+2\exp\left[\frac{-(x-2)^2}{2\beta}\right]-1\ , \tag{26}$$

where $\beta=0.297\,85$. This potential function is unbounded at the origin, has a local minimum $V(1)=0$ and a positive local maximum near $x=2$, and converges to a constant negative value for large x. Figure 4 plots $V(x)$ from (26).

We mimicked the preparation of a wave function which is initially localized in a neighborhood of the local

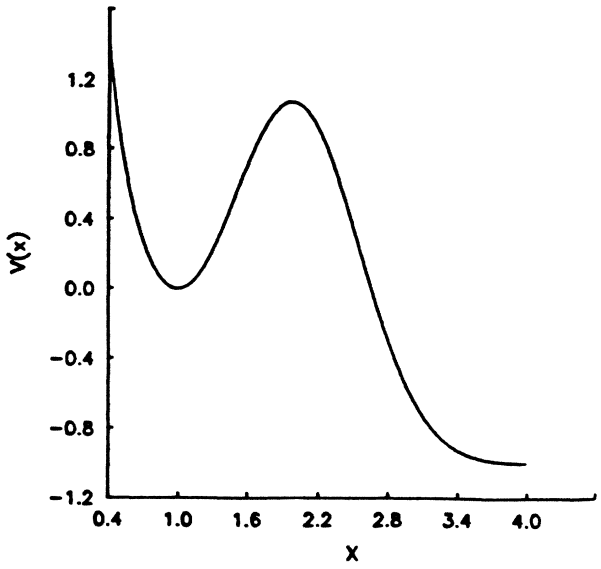

FIG. 4. Graph of potential (27) for the tunneling system.

mininum point $x=1$ by simply starting all 1000 sample trajectories at that point at $t=0$. Specifying the wave function is the same as specifying the current and osmotic velocity fields v and u,[4] which evolve according to a set of coupled partial differential equations[32] equivalent to the Schrödinger equation. The latter paper shows how to construct smooth initial data $v_0(x)$ and $u_0(x)$ for these equations such that for all times less than or equal to some fixed finite time t_0 (depending on $\hbar$), $v(x,t)$ and $u(x,t)$ stay uniformly close to $u_0(x)$ and $v_0(x)$ in the region where the potential is non-negative. In this fashion we may approximate the drift in (1). That the time t_0 must in general be finite we have shown by demonstrating that the evolution equations for v and u linearized about given steady-state solutions form an unstable (in fact, ill-posed) system[33] unless the steady state u is identically zero; the argument is straightforward but tedious and we do not present it here. We took the initial data as

$$v_0(x)=\begin{cases}0, & 0\le x\le 2.648\,017\,5\\ \sqrt{2\,|\,V(x)\,|}, & x>2.648\,017\,5\end{cases}$$
$$u_0(x)=\begin{cases}\sqrt{2V(x)}, & 0\le x\le 1\\ -\sqrt{2V(x)}, & 1\le x<2.648\,017\,5\\ 0, & x>2.648\,017\,5\ .\end{cases} \tag{27}$$

Jona-Lasinio, Martinelli, and Scoppola use a version of (27) in which v_0 and u_0 are interpolated smoothly to the vanishing parts of these functions in a small interval centered at the point where the graph of the potential crosses the x axis (about $x=2.648\,017\,5$ here); the length of the interpolation interval tends to zero as $\hbar$ approaches zero. For our time-discretized computational investigation this smoothness does not matter, since only a negligible error is incurred in the numerical trajectories by using (27) instead of the interpolated version, even though the actual v and u evolved from (27) generally do not remain near

these initial data.

The system will be assumed to have decayed when the particle, which begins in the region to the left of $x=2.648\,017\,5$, moves to the right of this point; since the potential continues to decrease to the right from there, the particle is then unlikely to go back into the interval to the left. Defining $P(t)$ (Ref. 32) as the probability that a particle starting at $x=1$ at time 0 exits the region (0,2.648 017 5) by or at time t, we choose $\hbar=0.1$ so that the exponent in the WKB-type estimate of $P(t)$ given in Ref. 32 is roughly of the order of unity.

Thus, using (27), we calculated 1000 trajectories for the approximate (for $t<t_0$) equation of motion

$$dq(t)=[v_0(q(t))+u_0(q(t))]dt+\sqrt{\hbar}\,dw(t)\ , \qquad (28)$$

with time step size $\delta t=0.01$ and initial value $q(0)=1$. For each such sample path the time when it went beyond $x=2.648\,017\,5$ was recorded, and then we added up the number of these exit times that are less than or equal to $5n$ time units for $n=0,1,2,\ldots,100$ and divided the result by the total number of trajectories. The curve graphed from the latter-computed approximation to $P(t)$ in Fig. 5, an approximation to $P(t)$, is highly accurately fit by the following exponential form:

$$P(t)=1-\exp[-(0.0122)t]\ . \qquad (29)$$

The inverse of the coefficient 0.0122 in the exponent in (29) is an empirical estimate ($\tau=81.9$) for the lifetime of this unstable system.

In Fig. 6(a) we graph one tunneling trajectory for this system, and in Fig. 6(b) the corresponding particle energy $\frac{1}{2}(v_0^2+u_0^2)+V$ is plotted. It can be seen that the energy is always non-negative, even when the particle is crossing the barrier.

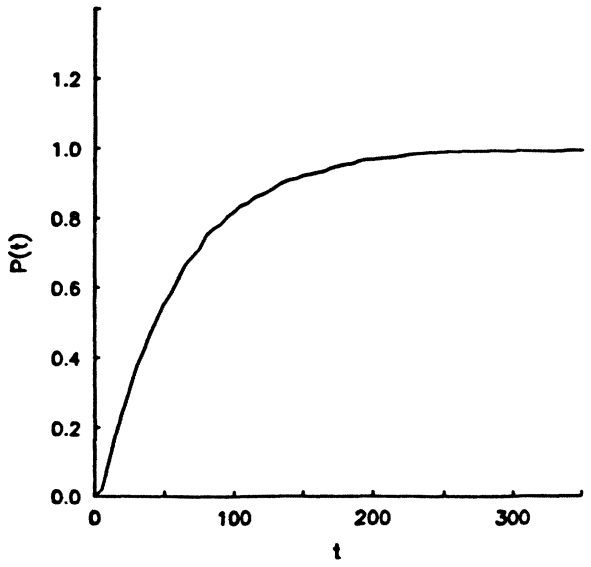

FIG. 5. For the tunneling system with potential (27), number of trajectories with time increment 0.01, starting with $x=1$, that have decayed by time t, divided by the total number of trajectories (1000).

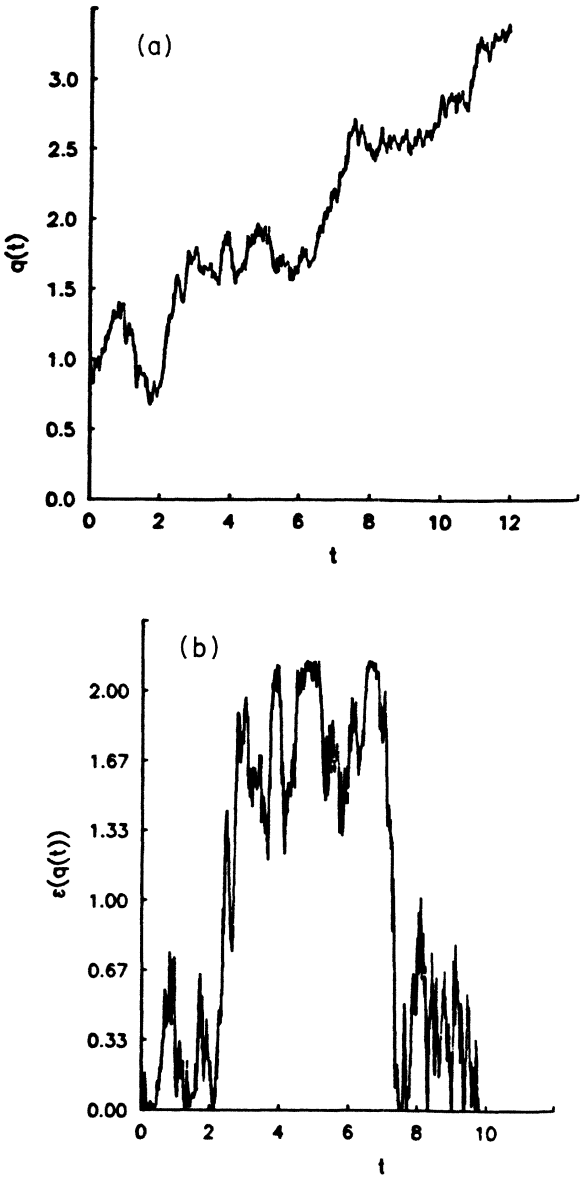

FIG. 6. For the tunneling system with potential (27); (a) the single tunneling trajectory with time increment 0.01, $q(0)=1$; (b) the energy of the particle with trajectory (a) as a function of time.

VI. QUANTUM CHAOS AND STOCHASTIC MECHANICS

Researches into quantum chaos have hitherto been hampered by a dearth of unambiguous criteria indicating the presence or absence of chaos in quantum dynamics. The latter difficulty arises from conventional quantum theory's complete specification of the state by the wave function, so different from the case for classical systems, and the related lack of particle trajectories. This raises the intriguing idea that quantum chaos could be investigated by studying the sample path behavior of the relevant Nelson diffusion process. This possibility is explored here, but we shall see that no definitive con-

clusions can be drawn at this point.

In this section we consider sample trajectories in stochastic mechanics as a means of looking for chaos in a system whose classical description is chaotic. Specifically, we seek to discover whether the paths of the Nelson diffusion process beginning at two neighboring configuration points diverge exponentially in this situation, as the corresponding classical trajectories in phase space do. Their doing so could turn out to be a useful criterion for quantum chaos.

The system we examine is the periodically driven pendulum or rotor studied by Casati *et al.*,[11] which classically exhibits chaotic behavior when the period of the perturbation exceeds a certain threshold and whose quantum version also shows signs of chaos for some values of its defining parameters. This system is not conservative, so its quantum version does not have to be quasiperiodic.[12] In units such that the mass, length, and fundamental angular frequency of the pendulum are all unity, the wave function, expanded in the basis of unperturbed rotor eigenfunctions $(2\pi)^{-1/2}e^{in\theta}$ is

$$\psi(\theta,t)=\frac{1}{\sqrt{2\pi}}\sum_{n=-\infty}^{\infty}A_n(t)e^{in\theta}, \tag{30}$$

where the coefficients $A_n(t)$ evolve in the time between applications of the periodic perturbation according to

$$A_n(t+\tau)=A_n(t)\exp\left[-\frac{in^2\hbar\tau}{2}\right], \tag{31}$$

and instantaneously at the time jT of a perturbing kick by

$$A_n(jT+)=\sum_{k=\infty}^{\infty}A_k(jT-)i^{n-k}J_{n-k}\left[\frac{1}{\hbar}\right]. \tag{32}$$

Here $\hbar$ is a parameter, T is the period of the externally applied δ-function perturbation, and the J_{n-k}'s are Bessel functions. Calculating the forward drift from (30) using (3), we obtain

$$b(\theta,t)=(\mathrm{Re}+\mathrm{Im})\left[\frac{i\sum_{n=-\infty}^{\infty}nA_n(t)e^{in\theta}}{\sum_{n=-\infty}^{\infty}A_n(t)e^{in\theta}}\right]. \tag{33}$$

The coefficients we employed were calculated by starting at time 0 with $A_0(0)=1$ and all other $A_n(0)$'s equal to zero, and by making use in (32) of the fact[11] that $J_k(1/\hbar)$ is negligible for $2/\hbar \ll k$. We utilized the IMSL routine MMBSJN to compute values of Bessel functions.

Taking $\delta t=0.02$, we integrated two sets of trajectories, 100 in each, with initial value $\theta_1(0)=3.14$ for the first set and $\theta_2(0)=\pi$ for the second, for 24 time units. The period of the perturbation was taken to be $T=2$, and we put $\hbar=0.05$; these parameter values correspond to the situation in Ref. 11 in which the quantum motion has numerous chaotic features. Conditioning the diffusion process to begin at two nearby points, we averaged each of the two families of trajectories $\theta_1(t)$ and $\theta_2(t)$ and took the difference

$$d(t)=\langle\theta_2(t)\rangle-\langle\theta_1(t)\rangle \tag{34}$$

between the resulting approximate conditional mean paths. We do not restrict $\theta(t)$ to lie between 0 and 2π and thus do not identify two such angles if they differ by an integer multiple of 2π.

In Fig. 7 the mean difference (34) between the paths is graphed over the whole time interval [0,24], and in Fig. 8 this difference is graphed over the interval [0,6]. In each of these plots the instantaneous and often radical alteration in the motion induced by a δ-function kick is evident.

The interpretation of the results portrayed in Figs. 7 and 8 in terms of exponential divergence of initially neighboring trajectories is problematical. On the one hand, before the first kick occurs the difference between the two conditional average motion grows linearly with time, between two given kicks the evolution of $d(t)$ is frequently basically linear, and a kick often completely reverses the direction of movement of $d(t)$; the latter quantity can go back through zero and diverge in the opposite direction. Thus one certainly cannot say unambiguously that the means of the two sets of paths diverge exponentially. On the other hand, a kick can substantially increase the absolute rate of change of $d(t)$, and $|d(t)|$ appears to grow exponentially in some regions spanning two or more δ perturbations. Perhaps there is clear exponential divergence over a much larger time scale; however, calculations on this system for such a time scale appear to require vast amounts of computer time because of the necessity of recomputing the Fourier coefficients $A_n(t)$ at each occurrence of the periodic perturbation.

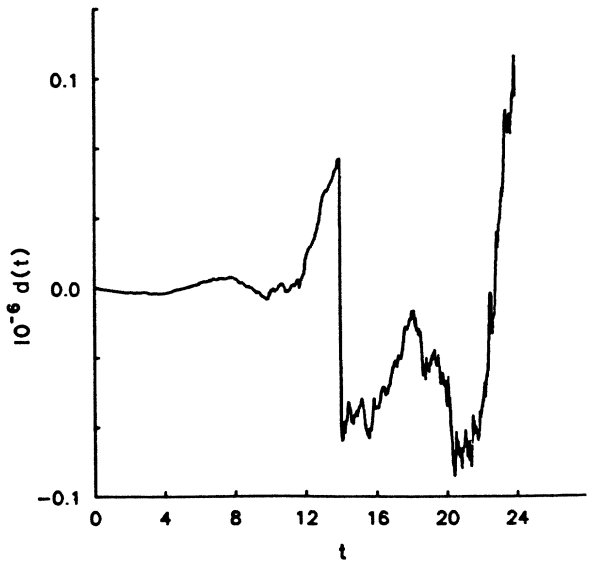

FIG. 7. For the periodically driven oscillator, the difference $d(t)$ of the means of two sets of 100 trajectories, one beginning at 3.14 and the other at 3.141 59.

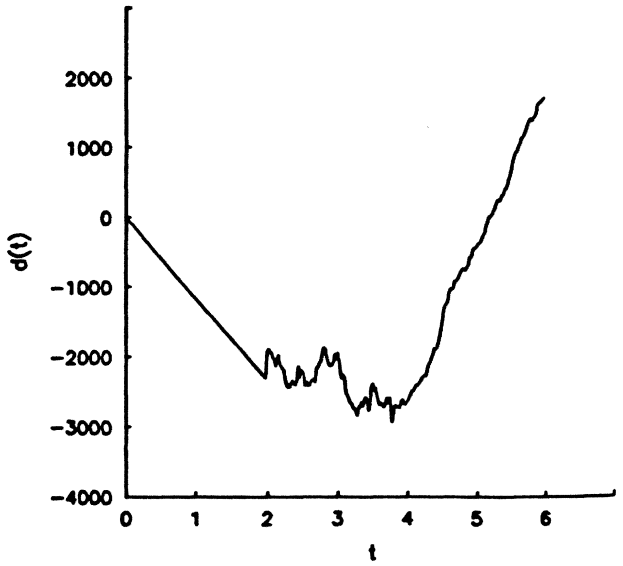

FIG. 8. Same as Fig. 7, restricted to time interval [0,6].

The question as to whether this stochastic mechanics approach is truly useful in elucidating quantum chaos can only be settled by further research on this and other systems.

VII. CORRELATED ELECTRON MOTION

The previous calculations dealt with only one particle. We now consider a two-particle system. The wave functions we use are analogs of ones describing H_2-like diatomic molecules when the Hamiltonian is independent of spin.

The simplest molecular orbital (MO) approach[34] to H_2 utilizes the product of two molecular orbitals, each of which is an equally weighted superposition of $1s$ atomic orbitals centered on the respective nuclei. We examine a model one-dimensional system with this kind of wave function, with the role of the atomic orbitals played by Gaussians. Specifically, let x_A and x_B be fixed given points representing nuclei, and let the "atomic" orbitals ψ_A and ψ_B be defined by, respectively,

$$\psi_A(x)=\frac{1}{\pi^{1/4}}\exp\left[\frac{-(x-x_A)^2}{2}\right] \tag{35}$$

and

$$\psi_B(x)=\frac{1}{\pi^{1/4}}\exp\left[\frac{-(x-x_B)^2}{2}\right] . \tag{36}$$

The corresponding MO wave function is then

$$\psi_{\mathrm{MO}}(x_1,x_2)=\frac{1}{2+2S}[\psi_A(x_1)+\psi_B(x_1)][\psi_A(x_2)+\psi_B(x_2)]$$

$$=\frac{1}{2+2S}[\psi_A(x_1)\psi_A(x_2)+\psi_A(x_1)\psi_B(x_2)+\psi_B(x_1)\psi_A(x_2)+\psi_B(x_1)\psi_A(x_2)] , \tag{37}$$

where S denotes the overlap integral[34] of the two orbitals,

$$S=\int_{-\infty}^{\infty}\psi_A(x)\psi_B(x)dx=\exp\left[-\frac{(x_A-x_B)^2}{4}\right] . \tag{38}$$

It is evident that in (37) the contribution of the "ionic" terms $\psi_A(x_1)\psi_A(x_2)$ and $\psi_B(x_1)\psi_B(x_2)$, each describing a situation in which both particles are near one nucleus or the other, is weighted equally with that of the "covalent" terms $\psi_A(x_1)\psi_B(x_2)$ and $\psi_B(x_1)\psi_A(x_2)$, which have one particle on one nucleus and the other particle on the other nucleus. Another model of a diatomic molecule is obtained from (37) by dropping the ionic terms entirely, leaving only the covalent ones. This leads to the Heitler-London (HL) (Ref. 34) approximate wave function which, using the orbitals (35) and (36), can be written as

$$\psi_{\mathrm{HL}}(x_1,x_2)=\frac{1}{(2+2S^2)^{1/2}}[\psi_A(x_1)\psi_B(x_2)+\psi_B(x_1)\psi_A(x_2)] . \tag{39}$$

In the ground state the electrons of H_2 are intuitively pictured as spending more time together near the same nucleus in the MO model than in the HL model. Conversely, the motion of the two electrons should be more anticorrelated in the HL model in the sense that if the electron on one of the nuclei moves to the other nucleus, then the other electron tends to get out of its way and go to the nucleus where the first electron originally was located. We now wish to compare the behavior of stochastic mechanical trajectories for systems having wave functions of the forms (37) and (39), respectively, in order to verify these intuitive pictures.

We take the unit of time to be the period of oscillation of a classical harmonic oscillator, the ground state of whose quantum version has a wave function of the form (35) or (36); the unit of distance is then such that the constant in the exponent of the Gaussian harmonic-oscillator function[27] is unity. The MO function (37), being the product of two one-particle wave functions, is a noninteracting particle model.[34] Substituting (37) into (3) yields the result that each of the two particles independently executes the one-dimensional diffusion $q(t)$ satisfying the Langevin equation (1) with drift

$$b(x)=-\left[\frac{(x-x_A)\exp[-(x-x_A)^2/2]+(x-x_B)\exp[-(x-x_B)^2/2]}{\exp[-(x-x_A)^2/2]+\exp[-(x-x_B)^2/2]}\right]. \tag{40}$$

In the HL model, by contrast, the two particles are dynamically coupled together. Here the components of the drift corresponding to the coordinates of the two particles are found, using (3) and (39), to be

$$b_1(x_1,x_2)=-\left[\frac{(x_1-x_A)\exp\left[\frac{-(x_1-x_A)^2-(x_2-x_B)^2}{2}\right]+(x_1-x_B)\exp\left[\frac{-(x_1-x_B)^2-(x_2-x_A)^2}{2}\right]}{\exp\left[\frac{-(x_1-x_A)^2-(x_2-x_B)^2}{2}\right]+\exp\left[\frac{-(x_1-x_B)^2-(x_2-x_A)^2}{2}\right]}\right] \tag{41}$$

and

$$b_2(x_1,x_2)=-\left[\frac{(x_2-x_B)\exp\left[\frac{-(x_1-x_A)^2-(x_2-x_B)^2}{2}\right]+(x_2-x_A)\exp\left[\frac{-(x_1-x_B)^2-(x_2-x_A)^2}{2}\right]}{\exp\left[\frac{-(x_1-x_A)^2-(x_2-x_B)^2}{2}\right]+\exp\left[\frac{-(x_1-x_B)^2-(x_2-x_A)^2}{2}\right]}\right]. \tag{42}$$

A larger value of S implies that it is more likely that a particle initially near one of the nuclei will move near the other nucleus. Choosing the centers of the Gaussians (35) and (36) to be $x_A=-1$ and $x_B=1$, respectively, we find that the overlap integral (38) has the reasonable value $S=\exp(-1)$. For each model we first integrated two single sample trajectories for $q_1(t)$ and $q_2(t)$, with $q_1(0)=-1$ and $q_2(0)=1$ in each case, from $t=0$ to $t=12$, using (40), (41), and (42) respectively. The time step size was taken to be $\delta t=0.01$. The MO results are plotted in Fig. 9 and the HL results in Fig. 10. It can be seen immediately that the HL trajectories are more anticorrelated than the MO ones; although due to random fluctuations sometimes the HL trajectories briefly appear uncorrelated or even positively correlated. It is interesting to notice the HL particles switching together to opposite sides of the origin in Fig. 10.

Next, with the same parameter values, we integrated two families of 10 000 pairs of such trajectories, one set each for the MO and the HL situations, distributing the initial points in both cases according to the left-hand orbital (35) for $q_1(0)$ and according to the right-hand orbital (36) for $q_2(0)$. The joint probability densities of $q_1(t)$ and $q_2(t)$ obtained by squaring (37) and (39) both give zero as the mean position of either particle at all times. We therefore approximated the correlation function of the two particles' positions by simply averaging the prod-

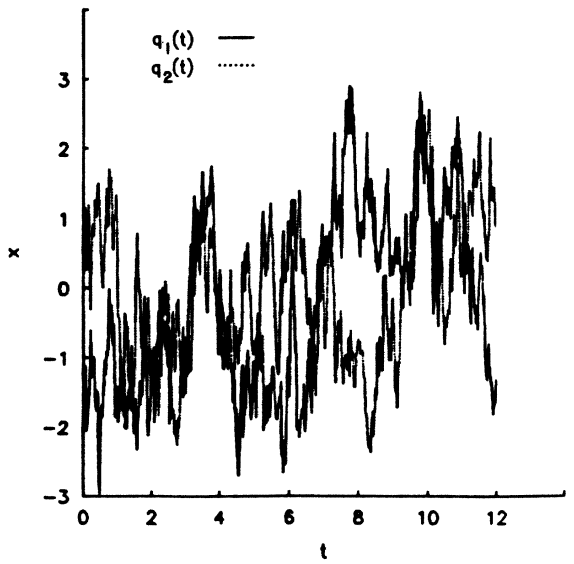

FIG. 9. For the one-dimensional correlated electron motion problem, two molecular orbital (MO) trajectories with time increment 0.01, one beginning at $x=-1$, the other at $x=1$.

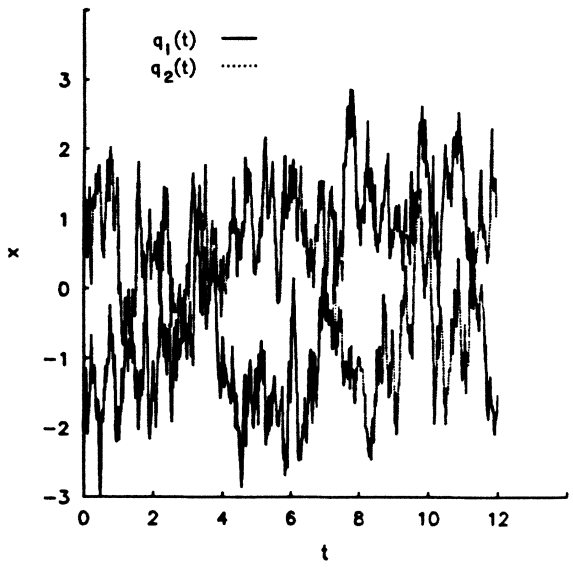

FIG. 10. For the one-dimensional correlated electron motion problem, two Heitler-London (HL) trajectories with time increment 0.01, one beginning at $x=-1$, the other at $x=1$.

uct $q_1(t)q_2(t)$ at each of the 1200 discrete times in the latter two calculations, graphing the MO correlation in Fig. 11 and the HL correlation in Fig. 12. The MO correlation jumps up quickly and hovers just below 0, whereas the HL correlation jumps down and hovers not far above -1. Thus the HL system is much more negatively correlated than the MO system, which is virtually uncorrelated. These results confirm in dramatic fashion the intuition behind the MO and HL models of H_2-like molecules.

Although these two one-dimensional pictures of H_2 are not realistic, the two models do contain all the important features connected with the correlation comparisons we wished to make. Similar phenomena to the ones discussed here should be observed in a stochastic mechanical treatment of the MO and HL models of the hydrogen molecule itself. The existence of particle trajectories in stochastic mechanics enables us to analyze quantitatively the electron exchange process, which can only be vaguely expressed within conventional quantum theory.

VIII. INFORMATION ON EXCITED STATES IN THE GROUND STATE

The Schrödinger equation can trivially be solved algebraically for the potential in terms of the ground-state wave function. Thus all information about the motion of the system in any of its excited states is contained in the motion of its ground state alone. In this section we show one way to utilize this idea and, in addition, establish a connection with a certain filter of statistical communication theory.[35]

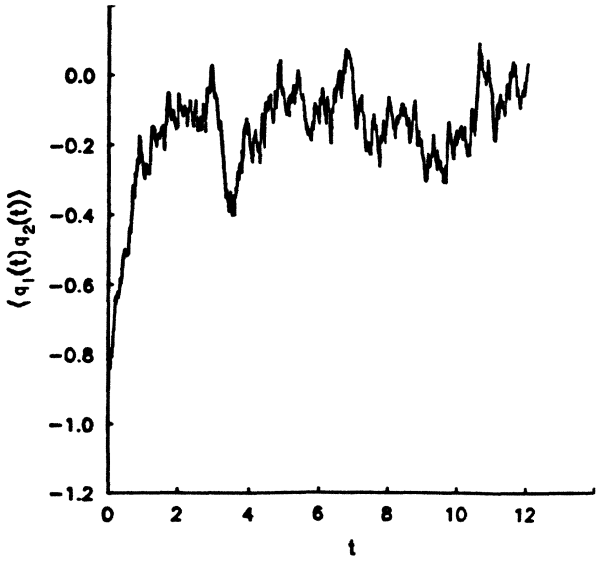

FIG. 11. For the one-dimensional correlated electron motion problem, correlation between two sets of 10 000 MO trajectories with time increment 0.01 and initially distributed, according to Gaussian orbitals (35) and (36) centered at $x=-1$, and $x=1$, respectively.

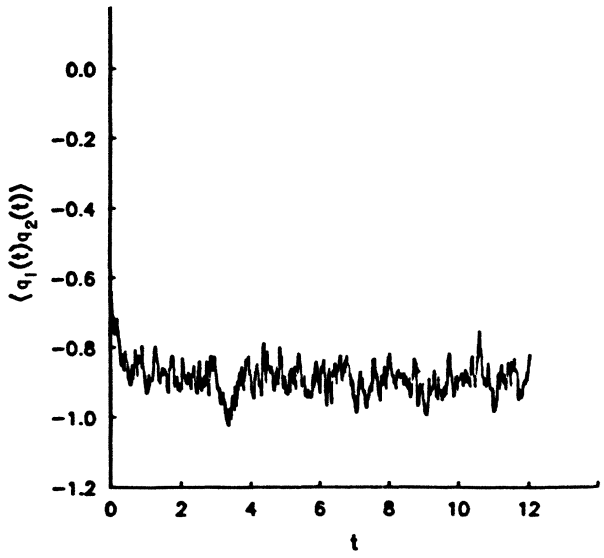

FIG. 12. For the one-dimensional correlated electron motion problem, correlation between two sets of 10 000 HL trajectories with time increment 0.01 and initially distributed according to Gaussian orbitals (35) and (36) centered at $x=-1$ and $x=1$, respectively.

Suppose the Hamiltonian operator $H=-\frac{1}{2}\nabla^2+V(x)$ on the Hilbert space $L^2(dx)$ has the bound-state eigenfunctions $\psi_0,\psi_1,\psi_2,\ldots$, with corresponding discrete spectrum $0=\varepsilon_0<\varepsilon_1<\varepsilon_2<\cdots$, where the energy scale has been adjusted such that the lowest eigenvalue of H is zero. Then H is equivalent via the unitary transformation $\hat{H}=\psi_0^{-1}H\psi_0$ to the self-adjoint operator $\hat{H}=-\frac{1}{2}\nabla^2-u\cdot\nabla$ on the Hilbert space $L^2(\rho_0 dx)$ of square-integrable functions with respect to the weight function equal to the ground density $\rho_0=\psi_0^2$;[1,4] u here is the osmotic velocity.[1] The latter operator is the infinitesimal generator[1,14] of the Markovian semigroup[1]

$$(P^t f)(x)=\mathrm{E}[f(q(t))\mid q(0)=x]=(e^{-t\hat{H}}f)(x)\ . \tag{43}$$

This semigroup describes the time evolution of the conditional expectation, given the initial value $q(0)$ of an arbitrary function of the stationary Markov diffusion process associated with any of the bound eigenstates of H.[36] If the set $\{\psi_0,\psi_1,\psi_2,\ldots\}$ is an orthonormal basis for $L^2(dx)$, then clearly $\{1,f_1f_2,\ldots\}$ is an orthonormal basis for $L^2(\rho_0 dx)$, where the nth eigenfunction f_n of the transformed operator $\hat{H}$ satisfies $f_n=\psi_0^{-1}\psi_n$.

Now, given the arbitrary function ψ in $L^2(dx)$, or equivalently the function $f=\psi_0^{-1}\psi$ in $L^2(\rho_0 dx)$, we can write $f=\sum_{n=0}^{\infty}\alpha_n f_n$ by completeness of the f_n; then let us expand the correlation function

$$\mathrm{E}[f(q(0))f(q(t))]\quad (t>0)\ ,$$

using the semigroup relation (43) and the orthonormality of the f with respect to ρ_0, as follows:

$$\mathrm{E}[f(q(0))f(q(t))]=\mathrm{E}\left[\left[\sum_{n=0}^{\infty}\alpha_n f_n(q(0))\right]\left[\sum_{m=0}^{\infty}\alpha_m e^{-t\hat{H}}f_m(q(0))\right]\right]$$
$$=\sum_{n,m=0}^{\infty}\alpha_n\alpha_m e^{-\varepsilon_m t}\int f_n(x)f_m(x)\rho_0(x)dx=\sum_{n=0}^{\infty}\alpha_m^2 e^{-\varepsilon_n t}. \tag{44}$$

Also employed in deriving this result are the Markov property of q and the fact that the expectation of a conditional expectation is the ordinary, unconditional expectation.[14] All the relevant series converge for $t\geq 0$ because f is square integrable and because of the decaying exponential factors in (44). It is easy to see that

$$\lim_{t\to\infty}\mathrm{E}[f(q(0))f(q(t))]=\alpha_0^2. \tag{45}$$

The correlation function $\mathrm{E}[f(q(0))f(q(t))]$ can in general be approximated by generating trajectories numerically, evaluating $f(q(0))f(q(t))$ for each one, and averaging; see (7). Now, subtracting α_0^2 from the correlation function (44) and using a similar argument to the one leading to (45), we get the leading term at large times,

$$\mathrm{E}[f(q(0))f(q(t))]-\alpha_0^2\sim\alpha_1^2 e^{-\varepsilon_1 t}. \tag{46}$$

By calculating the left-hand side of (46) for an interval of large times, where it would approximate the right-hand side, and then taking the logarithm, one obtains an estimate of the first excited energy eigenvalue ε_1. By repeating this process, one can successively estimate the higher energies. We note that if f is orthogonal to the nth eigenfunction f_n, then clearly the nth term in the series (44) is zero; this fact could be useful in choosing an appropriate function f for carrying out the calculations just described. This technique will be difficult to implement for a set of near-degenerate levels.

As a simple example that can be done analytically, we consider the one-dimensional harmonic oscillator with Hamiltonian $H=-\frac{1}{2}(\partial^2/\partial x^2)+\frac{1}{2}x^2-\frac{1}{2}$. Choosing ψ to be the generating function[27]

$$\psi(x)=\pi^{-1/4}\exp(-\tfrac{1}{2}x^2-\tfrac{1}{2}a^2+\sqrt{2}xa)=\sum_{n=0}^{\infty}\frac{a^n}{\sqrt{n!}}\psi_n(x) \tag{47}$$

for the normalized eigenfunctions ψ_n, where $\alpha_n=a^n/\sqrt{n!}$ and $a=$const, we have the correlation function expansion

$$\mathrm{E}[f(q(0))f(q(t))]=\sum_{n=0}^{\infty}\left[\frac{a^n}{\sqrt{n!}}\right]^2 e^{-nt}. \tag{48}$$

One sees immediately that following the above procedure leads directly to the eigenenergies $0,1,2,\ldots$.

Each of the exponential terms in the expansion (44) is the correlation function of the output of an RC low-pass filter subjected to a white-noise input with power spectral density $2\nu/\sqrt{2\pi}$, with the energy eigenvalue ε_n corresponding to the inverse of the product RC of the resistance R and the capacitance C.[35] Thus, by the orthonormality of the basis functions f_n, the correlation function is that of the (possibly infinite) linear combination $f(q(t))=\sum_n\alpha_n f_n(q(t))$ of such outputs $f_n(q(t))$. The Fourier transform

$$\frac{2}{\sqrt{\pi}}\mathrm{Re}\int_0^{\infty}\mathrm{E}[f(q(0))f(q(t))]e^{-i\omega t}dt$$
$$=\left[\frac{2}{\pi}\right]^{1/2}\sum_{n=1}^{\infty}\frac{\alpha_n^2\varepsilon_n}{\varepsilon_n^2+\omega^2} \tag{49}$$

of $\mathrm{E}[f(q(0))f(q(t))]$ is the power spectral density of the output process $f(q(t))$. Thus $f(q(t))$ has a peak in its power spectrum at zero frequency. In particular, if one takes f to be the eigenfunction f_n alone, then one obtains a low-pass filter with the half-maximum of its power spectrum at $\omega=\pm\varepsilon_n$. This provides the intuitively appealing interpretation of the Nelson stochastic process for a quantum system with a stationary wave function as the output of a certain filter which preferentially passes low frequencies and whose tendency to pass higher frequencies rises with the energy eigenvalue, where the input to the filter is just the background field of Brownian quantum fluctuations. Mitter[37] has established other connections between stochastic mechanics and filter theory.

The method of this section is conceptually similar to the projection method sometimes used with the Ritz principle[38] (i.e., take a trial function, project off ψ_0, and optimize the result giving ψ_1, etc.). In this connection see also Ref. 39, in which arbitrary semiclassical trajectories are used to obtain excited energies and eigenfunctions.

IX. CONCLUSION

In this article we have performed a set of numerical stochastic mechanical calculations on representative quantum systems. The study of one-dimensional free motion showed that Shucker's infinite-time-limit definition of momentum can be employed in computational work by considering the relevant ratio for large enough times. Along these lines, numerical simulation of stochastic mechanical trajectories of scattering particles to study their asymptotic behavior for large times (when the influence of the potential becomes negligible) would be an interesting approach to quantum scattering problems. The old conundrum concerning whether a quantum particle in the two-slit diffraction experiment passes through one or both slits receives a resolution in the stochastic interpretation: each particle goes through just one of the slits, but the wave function leads to a drift which produces the interference pattern. The generated interference patterns, including those for which all particles pass through one slit even though both are open, were made from ensembles of finitely many numerically

calculated stochastic mechanical trajectories. Carrying Jona-Lasinio, Martinelli, and Scoppola's analysis a step further, we have demonstrated an approximately exponential decay of a specific unstable stochastic mechanical system. Using the periodically driven pendulum model of Casati, Chirikov, Casati, and Ford, we have found preliminary indications that exponential divergence of initially nearby configuration space trajectories may occur in a stochastic mechanical system whose classical counterpart is chaotic; this might prove to be a fruitful way of investigating quantum chaos. Next, we have shown that the correlation of the trajectories in one-dimensional analogs of the molecular orbital and Heitler-London models of diatomic two-electron molecules conforms with intuitive notions related to the degree of ionic character of the two models. Finally, we have indicated how the motion of the ground state of a system contains information about the energies of its excited states.

Thus stochastic mechanics has significant possible utility for the insightful understanding of the behavior of quantum systems. It would be of considerable interest to see larger-scale computations on realistic systems exploiting the same conceptual tools. Since the wave function will typically depend on certain parameters, sensitivity analysis may be useful in such investigations; see Ref. 40.

ACKNOWLEDGMENTS

The authors thank the U.S. Air Force Office of Scientific Research and the U.S. Office of Naval Research for support of the present work. Moreover, we express our deep gratitude to Edward Nelson, whose encouragement and suggestions have tremendously aided this project. In addition, we acknowledge helpful discussions with Hans Beumee, Dalcio Dacol, and Martin Kruskal.

[1]E. Nelson, *Dynamical Theories of Brownian Motion* (Princeton University Press, Princeton, NJ, 1967).
[2]E. Carlen, Commun. Math. Phys. **94**, 293 (1984).
[3]E. Carlen, Ph.D. thesis, Princeton University, 1984 (unpublished).
[4]E. Nelson, Phys. Rev. **150**, 1079 (1966).
[5]E. Nelson (unpublished).
[6]E. Nelson, *Quantum Fluctuations* (Princeton University Press, Princeton, NJ, 1985).
[7]G. C. Ghirardi, C. Omero, A. Rimini, and T. Weber, Riv. Nuovo Cimento **1**, 1 (1978).
[8]R. P. Feynman, Rev. Mod. Phys. **20**, 367 (1948).
[9]F. Guerra, Phys. Rep. **77**, 263 (1981).
[10]P. Biler, Lett. Math. Phys. **8**, 1 (1984).
[11]G. Casati, B. V. Chirikov, F. M. Izraelev, and J. Ford, in *Stochastic Behavior in Classical and Quantum Hamiltonian Systems,* edited by G. Casati and J. Ford (Springer-Verlag, Berlin, 1979), p. 334.
[12]R. Kosloff and S. A. Rice, J. Chem. Phys. **74**, 1340 (1981).
[13]K. Yasue and J.-C. Zambrini, Ann. Phys. **159**, 99 (1985).
[14]A. D. Wentzell, *A Course in the Theory of Stochastic Processes,* translated by S. Chomet (McGraw-Hill, New York, 1981).
[15]Z. Schuss, *Theory and Applications of Stochastic Differential Equations* (Wiley, New York, 1980).
[16]E. Helfand, Bell Syst. Tech. J. **58**, 2289 (1979).
[17]H. S. Greenside and E. Helfand, Bell Syst. Tech. J. **60**, 1927 (1981).
[18]D. J. Wright, IEEE Trans. Auto. Control, February 1974, p. 75.
[19]D. K. Dacol and H. Rabitz, J. Math. Phys. **25**, 2716 (1984).
[20]J. B. Anderson, J. Chem. Phys. **63**, 1499 (1975).
[21]D. S. Shucker, J. Func. Anal. **38**, 146 (1980).
[22]E. Nelson, in *Mathematical Physics VII,* Proceedings of the Seventeenth International Congress on Mathematical Physics, Boulder, 1984, edited by W. E. Brittin, K. E. Gustafson, and W. Wyss (North-Holland, Amsterdam, 1984), p. 509.
[23]D. de Falco, S. De Martino, and S. De Siena, Phys. Rev. Lett. **49**, 181 (1982).
[24]L. de la Pena-Auerbach and A. M. Cetto, Phys. Lett. A **39**, 65 (1972).
[25]S. Golin, J. Math. Phys. **26**, 2781 (1985).
[26]E. Schrödinger, Preuss. Akad. Wiss. Phys. Math **K1**, 296 (1930).
[27]A. Messiah, *Quantum Mechanics* (Wiley, New York, 1961), Vol. I.
[28]J. E. G. Farina, J. Phys. A **17**, 1473 (1984).
[29]C. Philippidis, C. Dewdney, and B. J. Hiley, Nuovo Cimento B **52**, 15 (1979).
[30]C. Dewdney and B. J. Hiley, Found. Phys. **12**, 27 (1982).
[31]D. Bohm, Phys. Rev. **85**, 166 (1952).
[32]G. Jona-Lasinio, F. Martinelli, and E. Scoppola, Lett. Nuovo Cimento, **34**, 13 (1982).
[33]E. Zauderer, *Partial Differential Equations of Applied Mathematics* (Wiley, New York, 1983).
[34]M. W. Hanna, *Quantum Mechanics in Chemistry,* 3rd ed. (Benjamin/Cummings, Menlo Park, CA, 1981).
[35]J. B. Thomas, *An Introduction to Statistical Communication Theory* (Wiley, New York, 1969).
[36]S. Albeverio and R. Hoegh-Krohn, J. Math. Phys. **15**, 1745 (1974).
[37]S. K. Mitter, Ric. Automatica, **10**, 479 (1979).
[38]N. DeLeon and E. J. Heller, J. Chem. Phys. **78(b)**, 4005 (1983).
[39]S. Mikhlin, *Variational Methods in Mathematical Physics* (Pergamon, Elmsford, NY, 1964).
[40]M. McClendon and H. Rabitz, following paper, Phys. Rev. A **37**, 3493 (1988).